URSI AP-RASC 2019, New Delhi, India, 09 - 15 March 2019

Spoof Surface Plasmon based Planar Terahertz Dielectric Sensor

Surya Prakash Singh*[(1), (2)], Nilesh Kumar Tiwari[(1)], and M. Jaleel Akhtar[(1)]
(1) Indian Institute of Technology Kanpur, Uttar Pradesh, India, 208016
(2) International Institute of Information Technology Bhubaneswar, Odisha, India, 751003

Abstract

A planar terahertz (THz) dielectric sensor based on spoof surface plasmon (SSP) is proposed. The sensor comprises of the coplanar waveguide (CPW) line at the top of the substrate, whereas the symmetric dual T-shape SSP line having defect is designed at the back of the substrate. The defect at the center provides the change in the momentum of SSP wave traveling on the symmetric dual T-shape SSP line, which causes a strong resonance and hence localization of the field energy at the defect takes place. The strength of the localized field at the defect can be manipulated by managing the change in the momentum of SSP wave when it transmits through the defect from the T-shape SSP line. The placement of a dielectric sample at the defect location perturbs the localized field which helps to sense the dielectric property of the samples. Numerical simulations and optimization of the proposed THz sensor is carried out using the CST-MWS. The proposed SSP based THz dielectric sensor confirms the fully planar geometry unlike the earlier reported non-planar SSP dielectric sensor in THz frequency which basically ease its integration with the modern systems. The proposed sensor is numerically tested in the THz frequency region using a dielectric constant value corresponding to number of standard solid and liquid samples.

1. Introduction

The terahertz (THz) frequency spectrum covers the frequency range from microwave to infrared region. Thus, it exhibits the characteristic features of both infrared or visible light and radio waves. The terahertz spectrum is widely used in many industrial applications such as material characterization, security scanning, biomedical imaging, and defect location in artifacts due its various unique features. The THz based material characterization technique proves to be suitable for non-destructive testing as THz signal easily passes through the most of the dielectric materials [1]. The THz spectrum is safer to be used for security scanning and biomedical imaging applications due to its lower quantum energy of THz photons [2]. Moreover, the relatively smaller wavelengths at THz frequency results into higher resolution as compared to the existing microwave and millimeter wave imaging techniques [3]. Apart from these features, the THz spectrum uniquely holds the finger-prints for a range of reagents, which is one of the important aspect of material spectroscopy, thus makes the THz radiation suitable for dielectric testing of various types of test specimens [4]. Nowadays, the THz spectrum is getting the attention of researchers due to the above mentioned specific features [5]. Therefore, it is extremely important to know the dielectric property of the materials in THz frequency region so that efficient systems for the above mentioned applications can be developed. The dielectric testing and material characterization at THz frequency is mostly done in free space by using the time domain or frequency domain spectroscopic techniques [6]. In many cases, it is not suitable to use the free space material characterization techniques to test the samples due to the practical limitations such as sample size, diffraction limit and low power signals, etc., therefore the need of sensors has arisen.

The concept of spoof surface plasmon (SSP) has been used frequently to design various THz dielectric sensors due to its excellent ability to trap the electromagnetic (EM) wave within the subwavelength region [7]. However, the earlier designed SSP sensor are non-planar in nature, therefore they might not be suitable for integrated THz sensing systems [8-10]. Here, it is worth mentioning that the higher radiation and propagation loss at high frequency regime limits the use of conventional planar microstrip technology based structures. Hence, the designing of planar sensors at very high frequency by using the concept of SSP can be a good idea as the wave remains tightly confine to the dielectric and metal interface, which results low ohmic and radiation loss [11]. The dispersion property of the SSP unit cell can be modified by altering the geometrical parameters of the unit cell, thus the propagation and confinement of the EM field in the SSP unit cell can easily be engineered [12]. From the dielectric sensing application point of view, we need a strong localization of SSP field signal so that a better interaction between the field and sample under test can take place. In this article, a detailed analysis of dispersion characteristic of SSP cell and its effect on the localization of field is discussed. To the best of authors' knowledge, the concept of SSP for dielectric sensing application using the planar structures has not reported in literature.

In this work, a coplanar waveguide (CPW) THz sensor based on SSP concept is presented. The top of the sensor consists the conventional CPW line which helps to excite the SSP wave through magnetic coupling in the symmetric dual T-shape SSP line present at the bottom of

the substrate. A defect is created at the center of the SSP line to generate the phase mismatch between the SSP wave traveling in the symmetric dual T-shape SSP line and defect cell. Due to the intentionally created phase mismatch, a strong resonance occurs and the transmitting energy associated to the SSP wave localizes at the defect. The localized field at the defect is optimized by properly choosing the physical parameters of the T-shape unit cell and defect cell. The eigenmode solver of the CST-MWS is employed to carry out the dispersion diagram analysis which basically helps to quantify the phase mismatch between the defect cell and the main symmetric dual T-shape unit cell. The electrically small defect region facilitates the strong electric field localization in its vicinity and hence it becomes possible to perform the dielectric sensing of relatively smaller volume dielectric samples. The Q-factor and the sensitivity of the numerically optimized SSP sensor is found to be 133 and 3.21, respectively, which is quite decent for dielectric sensing of low loss samples. Thereafter, the designed sensor is employed for the dielectric sensing of wide range of dielectric constant including the solid and liquid samples in the THz frequency region. The numerical analysis shows that the proposed SSP based planar THz sensor is able to differentiate between the dielectric samples with having closely distributed dielectric properties. At the end, a graphical curve between the permittivity of the test sample and resonant frequency is plotted to extract the permittivity of the unknown sample.

2. Dispersion Analysis

Fig. 2(a) and 2(b) show the symmetrical dual T-shape unit cell and defect cell, respectively and Fig. 2(c) shows the dispersion curves of both the unit cells. The dispersion plots presented in Fig. 2(c) helps us to understand the trapping of SSP field at the defect location. From the dispersion curves, it is observed that the SSP waves travelling in T-shape unit cell and defect cell has different phase and therefore the SSP wave, excited in the symmetric dual T-shape SSP line by the magnetic field of the CPW line, has to go for the phase change when it passes through the defect cell, located at the center of the SSP line. The change in the phase of the propagating SSP wave produces a resonance which helps to trap the transmitting energy at the defect location. The higher the phase mismatch between the main line SSP unit cell and defect cell, the higher the field localization, hence the shape and size of the SSP line unit cell and defect cell should be chosen such that it produces a high phase mismatch between cells.

From dispersion curves, it can clearly be observed that the phase mismatch in the SSP wave at symmetric dual T-shape unit cell and defect cell is high for the small size of defect, i.e., h = 0.3 mm, hence it is selected as the optimized height value for the vertical stub of the defect. The effect of h in trapping the field at the defect is also explained with the help of electric field plots in coming sub-section.

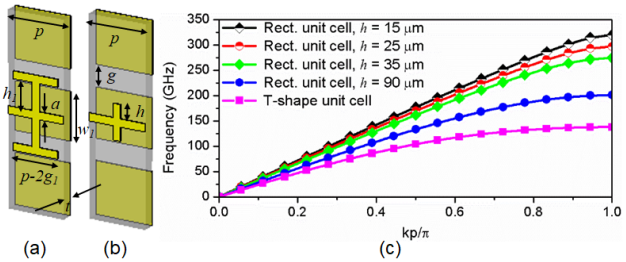

Figure 1. (a) symmetrical dual T-shape SSP unit cell, (b) symmetrical dual rectangular SSP unit cell, (c) dispersion plots corresponding to both the unit cell for fixed periodicity p = 150 μm.

Fig. 2 shows the numerical model of the proposed THz SSP planar dielectric sensor. The substrate material is 50 μm thick Rogers RT/Duroid 6010 and the thickness of the copper layer (σ = 5.8x10^7 S/m) is 200 nm. Fig. 2 shows the top view of SSP line with the defect at the center and the conventional CPW line can be observed at the back side of the SSP line. To maintain the 50 ohm characteristic of the line, the width of the signal line and gap between the signal line and ground of the CPW line are selected as 125 μm and 55 μm, respectively. The other optimized parameters of the designed SSP sensor are: L = 3000 μm, W = 1000 μm, a = 20 μm, g_1 = 15 μm, p = 150 μm, h = 15 μm, h_1 = 82.5 μm.

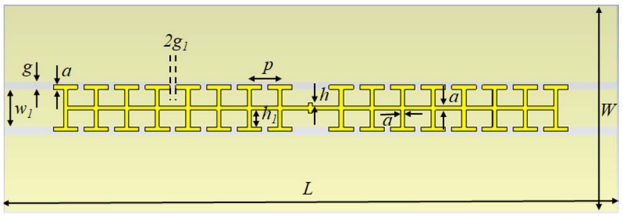

Figure 2. CST model of the proposed SSP line loaded CPW THz dielectric sensor.

Fig. 3 shows the magnitude electric field corresponding to the different values of h. It can be witnessed that the localized field is maximum for the smaller value of h, which is also evident from the dispersion curve analysis. As we can see that the major portion of the field concentrates around the defect and a small portion of the field spills around the adjacent unit cell, therefore the sample size is chosen as 3p x 3p (450 μm x 450 μm), so that it can cover the maximum part of trapped field for better material field interaction.

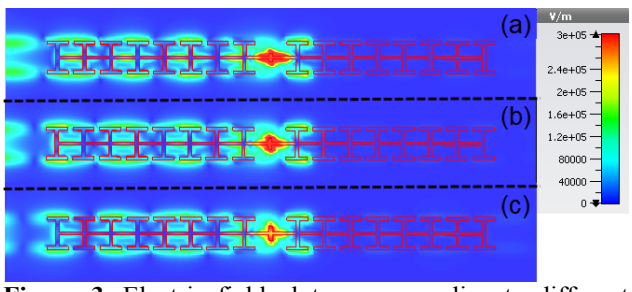

Figure 3. Electric field plots corresponding to different values of, h (a) h = 15 μm, (b) h = 25 μm, (c), h = 35 μm.

Fig. 4 shows the transmission response of the proposed SSP based THz sensor under no-load and load condition. From the transmission response, the quality factor and the sensitivity of the sensor (the percentage change in the resonance frequency for the unit change in the permittivity of the sample) is found to be 133 and 3.21, respectively.

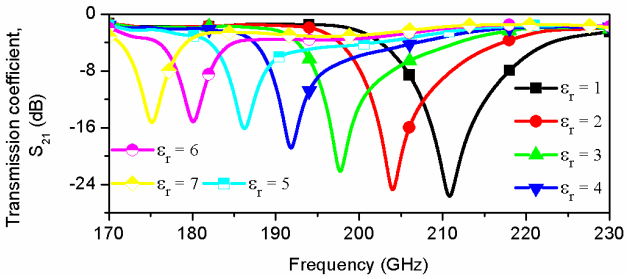

Figure 4. Transmission response of the sensor for no-load condition (ε_r = 1) and load condition (permittivity of sample varies from 2 to 7).

As we have discussed in the dispersion curve analysis that the shape and size of the SSP line unit cell and defect cell should be selected such that a maximum change in the momentum of the SSP wave can be achieved. We have designed another THz SSP sensor, shown in Fig. 5. In Fig. 5, the SSP line consists the symmetrical dual rectangular shape arrays, where the height of the rectangular vertical stub of the array is kept identical to the height of the T-shape unit cell.

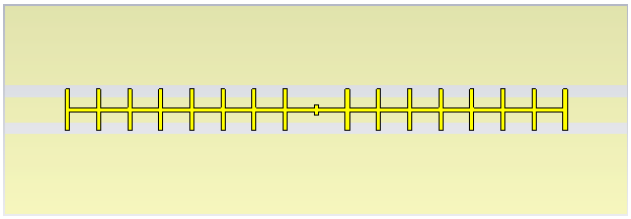

Figure 5. CST model of the SSP line loaded CPW THz dielectric sensor, here the SSP line consists the symmetrical dual rectangular arrays.

The transmission response of the designed sensor presented in Fig. 5 under no-load and load condition is shown in Fig. 6. From the transmission response, the calculated quality factor and sensitivity of the sensor comes 103 and 2.43, which are lower in comparison to the previous proposed sensor. The reason for low sensitivity of the later proposed sensor is because of small phase mismatch between the symmetrical dual rectangular SSP cell and defect cell in comparison to the symmetrical dual T-shape SSP cell. For further assistance, the trapped electric field at resonance frequency is plotted in Fig. 7. It can be clearly observed that the strength of the trapped electric field at the defect location is very low for the later designed sensor in comparison to the proposed T-shape SSP line loaded CPW sensor. Hence, there would be low interaction between the sample under test and trapped electric field for later designed sensor, i.e., low sensitivity. The sensitivity of the proposed SSP line loaded CPW sensors can be improved by selecting different SSP unit cell such as symmetrical dual dumbbell shape or symmetrical dual folded stub cell.

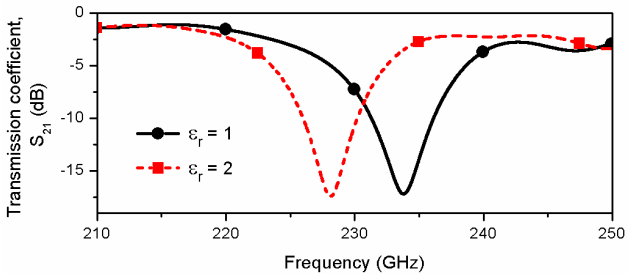

Figure 6. Transmission response of the second designed sensor under no load condition (ε_r = 1) and load condition (ε_r = 2).

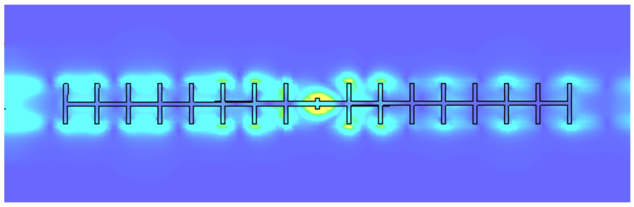

Figure 7. Electric field plot at the resonance frequency.

3. Dielectric Material Testing and Characterization

The proposed T-shape SSP line loaded CPW planar sensor is numerically tested for various dielectric samples. The transmission coefficients corresponding to the various samples under test with close permittivity values are shown in Fig. 8. It can be observed that the sensor is able to discriminate the dielectric samples of having close permittivity values, i.e., the proposed sensor can be deployed for dielectric testing and adulteration application where the adulterating sample has the similar dielectric property as the parent liquid sample.

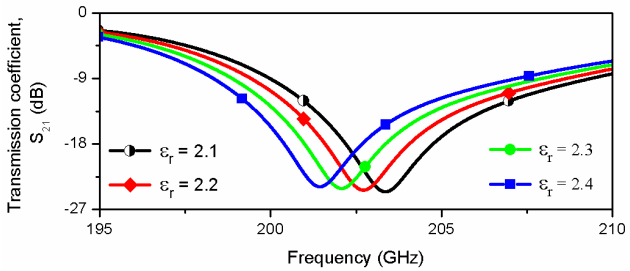

Figure 8. Transmission response of the sensor for samples with close permittivity value (permittivity of sample varies from 2.1 to 2.4).

Fig. 4 shows the transmission response for a wide range of permittivity samples. From this transmission coefficient plots, we can make another graphical plot which relate the permittivity of the sample under test and corresponding resonance frequency, shown in Fig. 9. From the plot shown in Fig. 9, an empirical relation is developed by using the curve fitting techniques which

correlate the resonance frequency and permittivity of the sample under test such as:

$$\varepsilon_r = -20.162 + 92.44*\exp(-0.007*f_r) \quad (1)$$

The permittivity of an unknown material can be easily determined from (1), once the resonant frequency of the unknown sample is determined by placing the sample on to proposed THz sensor.

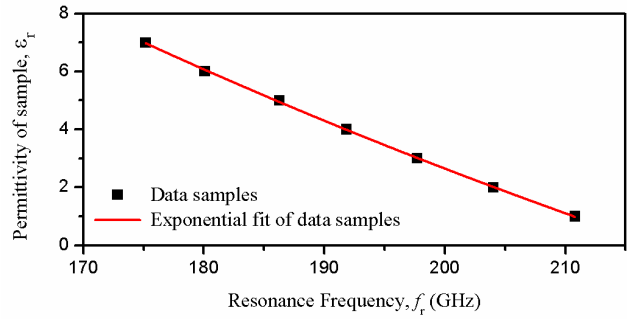

Figure 9. Exponential fit curve relating the sample permittivty and corresponding resonance frequency.

4. Conclusion

A SSP based planar THz dielectric sensor is proposed in this work, which consists the main CPW line at the top of the substrate and a SSP line with single defect at the back of the substrate. The tightly confined SSP wave travelling in the SSP line is trapped at electrically small region by creating a defect at the center which helps to sense the samples under test. The sensor is numerically tested for various permittivity values which shows that the proposed sensor has the ability to differentiate dielectric samples with close permittivity value and it also works for wide range of permittivity of samples. Thus the proposed sensor has potential to be employed in adulteration detection applications and non-destructive material characterization applications. The proposed THz sensor is fully planar in nature therefore it can be easily integrated with the conventional planar high frequency systems and components.

5. References

1. J. A. Hejase, P. R. Paladhi, and P. P. Chahal, "Terahertz characterization of dielectric substrates for component design and nondestructive evaluation of packages," *IEEE Transaction on Terahertz on Science and Technology*, **1**, 2011, pp. 1685–1694.
2. X. Shen, C. Dietlein, E. Grossman, Z. Popovic, and F.Meyer, "Detection and segmentation of concealed objects in terahertz images," *IEEE Transaction on. Image Processing*, **17**, 2008, pp. 2464–2475.
3. A. Dobroiu, C. Otani, and K. Kawase, "Terahertz-wave sources and imaging applications," *Measurement Science and Technology,* **17**, 2006, pp. R 161–R174.
4. J. F. Federici, et al., "THz imaging and sensing for security applications—Explosives, weapons and drugs," *Semiconductor Science and Technology*, **20**, 2005, pp. S266–S280.
5. J. Bianca Jackson, et al., "A survey of terahertz applications in cultural heritage conservation science," *IEEE Transaction on Terahertz on Science and Technology,* **1**, 2011, pp. 220–231.
6. J. A. Hejase, E. J. Rothwell, and P. Chahal, "Self-calibrating technique for terahertz time-domain material parameter extraction," *Journal of the Optical Society of America,A*, **2**8, 2011, pp. 2561–2567.
7. W. L. Barnes, A. Dereux, and T. W. Ebbesen, "Surface Plasmon subwavelength optics," *Nature*, **424**, 2003, pp. 824–830,.
8. P. Singh, "SPR Biosensors: Historical Perspectives and Current Challenges", *Sensor and. Actuators B Chemical,* **229**, 2016, pp. 110-130.
9. C. Lertvachirapaiboon et al., "Transmission surface plasmon resonance techniques and their potential biosensor applications", *Biosensors and Bioelectronics,* **99**, 2018, pp. 399–415.
10. H. Yao, S. Zhong, and W. Tu, "Performance analysis of higher mode spoof surface plasmon polariton for terahertz sensing" *Journal of Applied Physics,* **117**, 2015, pp. 133104-07.
11. Amin Kianinejad, Zhi Ning Chen, and Cheng-Wei Qiu, "Low-loss spoof surface plasmon slow-wave transmission lines with compact transition and high isolation," *IEEE Transactions on Microwave Theory and Techniques,* **64**, 2016, pp. 3078–3086.
12. J. B. Pendry, Martin-Moreno, and F. J. Garcia-Vidal, "Mimicking surface plasmons with structured surfaces," *Science*, **305**, 2004, pp. 847-848.